Active Site Residues in *Mycobacterium tuberculosis* Pantothenate Synthetase Required in the Formation and Stabilization of the Adenylate Intermediate†

Renjian Zheng,‡ Tarum K. Dam,§ C. Fred Brewer,§ and John S. Blanchard*,‡

Departments of Biochemistry and Molecular Pharmacology, Albert Einstein College of Medicine, 1300 Morris Park Avenue, Bronx, New York 10461

Received February 12, 2004; Revised Manuscript Received April 13, 2004

ABSTRACT: Pantothenate synthetase (EC 6.3.2.1) catalyzes the formation of pantothenate from ATP, D-pantoate, and β-alanine in bacteria, yeast, and plants. The three-dimensional structural determination of pantothenate synthetase from *Mycobacterium tuberculosis* has indicated specific roles for His44, His47, Asn69, Gln72, Lys160, and Gln164 residues in the binding of substrates and the pantoyl adenylate intermediate. To evaluate the functional roles of these strictly conserved residues, we constructed six Ala mutants and determined their catalytic properties. The substitution of alanine for H44, H47, N69, Q72, and K160 residues in *M. tuberculosis* pantothenate synthetase caused a greater than 1000-fold reduction in enzyme activity, while the Q164A mutant exhibited 50-fold less activity. The rate of the isolated adenylation reaction in single turnover studies was also reduced 40−1000-fold by the replacement of one of these six amino acids with alanine, suggesting that these residues are essential for the formation of the pantoyl adenylate intermediate. The rate of pantothenate formation from the adenylate and β-alanine in the second half reaction could not be measured for the H44A, H47A, N69A, Q72A, and K160A mutants and was reduced 40-fold in the Q164A mutants. The activity of the K160C mutant enzyme was markedly enhanced by the alkylation of cysteine with bromoethylamine, further supporting the critical role of the K160 residue in pantoyl adenylate formation. Isothermal titration microcalorimetry analysis demonstrated that the substitution of either H47 or K160 for Ala resulted in a decreased affinity of the enzyme for ATP. These results indicate that the highly conserved His44, His47, Asn69, Gln72, Lys160 and residues are essential for the formation and stabilization of pantoyl adenylate intermediate in the pantothenate synthetase reaction.

Pan[1] (vitamin B5) is a key precursor required for the biosynthesis of coenzyme A (CoA) and acyl carrier protein (ACP) (*1*). Both CoA and ACP are essential cofactors required for many cellular processes including fatty acid metabolism, cell signaling, and the biosynthesis of polyketides and nonribosomal peptides (*2*−*4*). The Pan biosynthetic pathway is best characterized in *Escherichia coli* and *Salmonella typhimurium* (Scheme 1). Pan is synthesized from α-ketoisovalerate, an intermediate in valine and leucine biosynthesis, in four steps (*5*, *6*). The genes encoding the enzymes involved in Pan biosynthesis from α-ketoisovalerate, *panB*, *panC*, *panD*, and *panE*, have been identified (*7*, *8*). Pan is synthesized in bacteria, yeast, and plants but not in mammals (*1*), suggesting that the enzymes involved in Pan biosynthesis are appropriate targets for the development of antibacterial agents. In support of this, Sambandamurthy and Jacobs (*9*) have reported that a Pan auxotrophic mutant of *Mycobacterium tuberculosis* is highly attenuated in immunocompromised mice and in immunocompetent mice, indicating that the biosynthesis of Pan is essential for the growth and virulence of *M. tuberculosis*.

PS (EC 6.3.2.1), encoded by the *panC* gene, catalyzes the formation of the amide bond of Pan from D-pantoate and β-alanine accompanied by the hydrolysis of Mg-ATP into AMP and Mg-PP_i (*10*). PS has been purified and partially characterized from *M. tuberculosis*, *E. coli*, *Lotus japonicus*, and *Oryza sativum* (*11*−*13*). The three-dimensional structures of PS from both *E. coli* and *M. tuberculosis* have been recently reported and reveal that it is a member of the cytidylyltransferase family of enzymes (*14*, *15*). We have previously cloned, expressed, purified, and kinetically characterized PS from *M. tuberculosis* (*11*). The enzyme is a homodimer with a subunit molecular mass of 33 kDa. The kinetic mechanism of the *M. tuberculosis* PS is Bi Uni Uni Bi Ping Pong, with ATP binding followed by D-pantoate binding, release of PP_i, binding of β-alanine, and finally the release of Pan and AMP. On the basis of this kinetic mechanism, the overall reaction consists of two sequential steps, pantoyl adenylate formation and the subsequent nucleophilic attack on the mixed anhydride by β-alanine to

† This work was supported by NIH Grant AI33696.

* To whom correspondence should be addressed. Tel: 718-430-3096. Fax: 718-430-8565. E-mail: blanchar@aecom.yu.edu.

‡ Department of Biochemistry.

§ Department of Molecular Pharmacology.

[1] Abbreviations: PS, pantothenate synthetase; HP, D-(−)-pantoate; Pan, pantothenate; NADH, reduced β-nicotinamide adenine dinucleotide; IPTG, isopropyl-1-thio-β-D-galactopyranoside; SDS-PAGE, sodium dodecyl sulfate-polyacrylamide gel electrophoresis; HEPES, 4-(2-hydroxyethyl)-1-piperazineethanesulfonic acid; TEA, triethanolamine; ATP, adenosine 5′-triphosphate; AMP-CPP, α,β-methyleneadenosine 5′-triphosphate; AMP, adenosine 5′-monophosphate; PEI-F TLC, poly(ethylenimine)cellulose-F thin-layer chromatography; EDTA, ethylenediaminetetraacetic acid; NMR, nuclear magnetic resonance.

10.1021/bi049676n CCC: $27.50
Published on Web 05/11/2004

Scheme 1

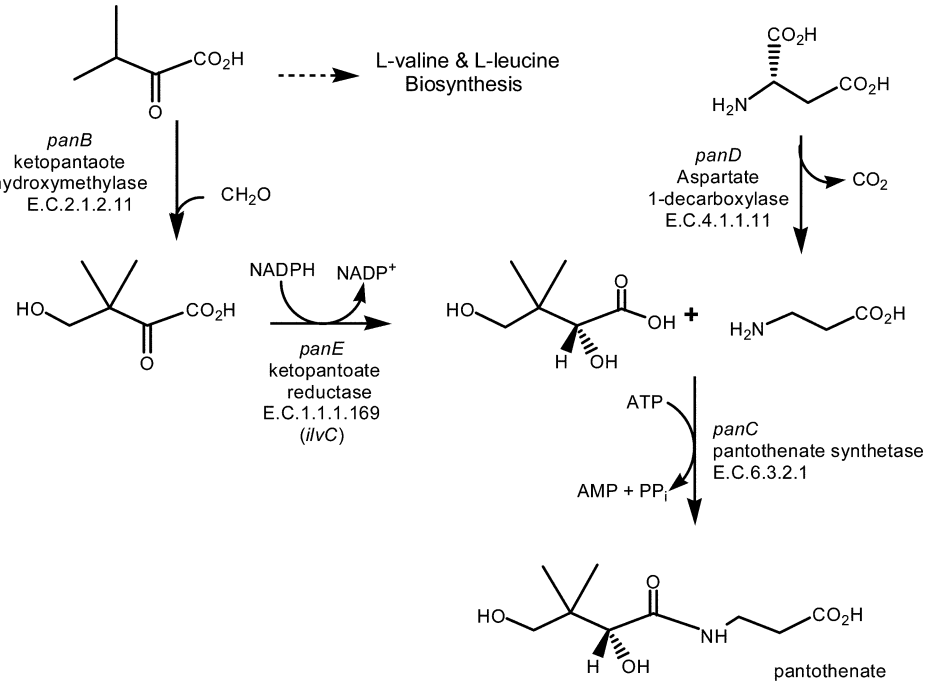

Scheme 2

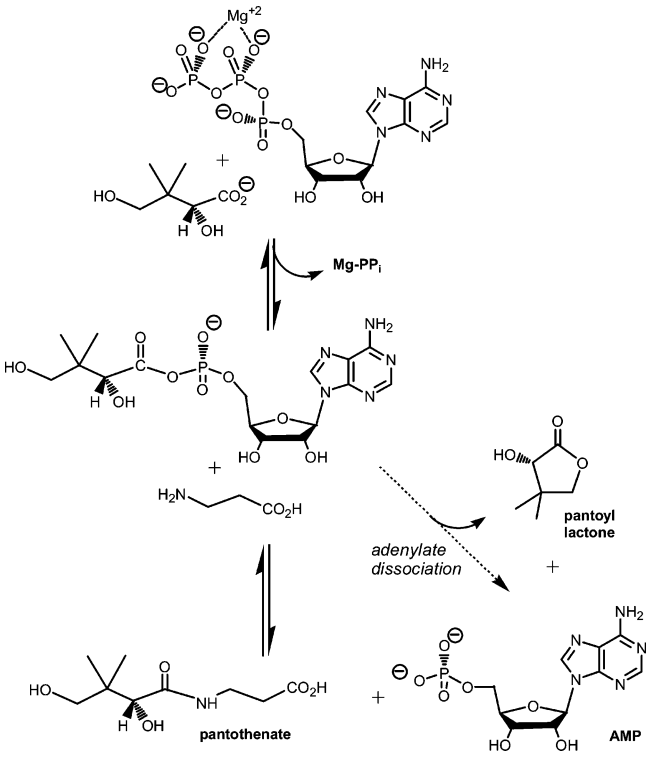

form Pan and AMP (Scheme 2). The formation of pantoyl adenylate, proposed as a required intermediate in the kinetic mechanism, was supported by ^{31}P NMR spectroscopy of the product, [^{18}O]AMP, produced by ^{18}O transfer to AMP from [carboxyl-^{18}O]pantoate (*11*). The reversibility of the formation of the pantoyl adenylate intermediate has been confirmed using positional isotope exchange methods (*16*). The formation of an acyl-adenylate intermediate has also been reported for malonyl-CoA synthetase and tyrosyl-tRNA synthetase (*17*, *18*). The three-dimensional structures of *M. tuberculosis* PS in complex with AMP-CPP, pantoate, and the pantoyl adenylate suggested roles for the completely conserved His44, His47, Asn69, Gln72, Lys160, and Gln164 residues in the binding of substrates and the pantoyl adenylate intermediate (*15*). To assess the functional roles of these residues in substrate binding and catalysis, we have constructed six alanine mutants and examined the catalytic effects on both the overall reaction and the isolated steps of adenylation and amide formation. Replacement by alanine of any of these six residues resulted in a significant decrease in catalytic efficiency, confirming their roles in substrate binding and adenylate formation and stability.

MATERIALS AND METHODS

Materials. NADH, IPTG, ATP, β-alanine, [^{14}C]β-alanine, myokinase (rabbit muscle), pyruvate kinase (rabbit muscle), and lactate dehydrogenase (rabbit muscle) were purchased from Sigma. All restriction enzymes and T4 DNA ligase were obtained from New England Biolabs. *Pfu* DNA polymerase was from Stratagene. pET23a (+) plasmid and *E. coli* strain BL21 (DE3) were obtained from Novagen. All chromatographic supports were from Pharmacia. PEI-F TLC plates were obtained from EM Science. [γ-^{32}P]ATP (6000 Ci/mmol) was from NEN DuPont Corp. Pantoyl lactone and other chemicals were obtained from Aldrich. Pantoic acid was prepared from pantoyl lactone using NaOH as previously described (*19*).

Cloning and Expression of Wild-Type (WT) and Mutants of M. tuberculosis PS. The *panC* gene (Rv3602c), encoding PS, was obtained by polymerase chain reaction amplification of the gene from genomic DNA of *M. tuberculosis* as previously described (*11*). The singly mutated genes corresponding to H44A, H47A, K160A, K160C, N69A, Q72A, and Q164A were generated using the QuickChange site-directed mutagenesis kit (Stratagene) according to the manufacturer's instructions and pET23a(+):*panC* as the template. The mutant genes were sequenced in their entirety to ensure that no unexpected mutations occurred. Both WT

Table 1: Steady State Kinetic Parameters of WT and Mutants of *M. tuberculosis* PS

			[^{14}C]β-alanine	
PS	k_{cat} (s^{-1})[a]	k_{cat} (s^{-1})[b]	K_m (mM)[b]	k_{cat}/K_m ($M^{-1}\,s^{-1}$)[b]
WT	0.99 ± 0.01	1.01 ± 0.05	0.27 ± 0.03	3.7×10^3
H44A	0.041 ± 0.002	<0.001		
H47A	0.032 ± 0.003	<0.001		
K160A	0.0055 ± 0.0003	≪0.001		
K160C	0.0040 ± 0.0002	≪0.001		
K160C$_{-CH_2CH_2NH_2}$	0.095 ± 0.009	0.010 ± 0.001	0.09 ± 0.03	111
N69A	0.048 ± 0.001	<0.001		
Q72A	0.075 ± 0.002	<0.001		
Q164A	0.149 ± 0.001	0.020 ± 0.003	0.3 ± 0.1	67

[a] Determined using the spectrophotometric coupled enzyme assay to monitor AMP formation. [b] Determined using isotopic assay measuring [^{14}C]Pan formation from pantoate, ATP, and [^{14}C]β-alanine.

and mutant genes were expressed in the *E. coli* strain BL21 (DE3). The BL21 (DE3) cells containing pET23a(+):*panC* or mutant genes were grown at 37 °C to an A_{600} of 0.5 in LB medium containing 50 μg/mL carbenicillin. IPTG (0.5 mM) was added to the culture, and growth was continued for an additional 4 h at 37 °C for the WT gene or overnight at 18 °C for mutant genes.

Purification and Analysis of WT and Mutants of the Recombinant PS. Cells (8−10 g) were suspended in 60 mL of 40 mM TEA-HCl, pH 7.8, containing protease inhibitors (Boehringer Mannheim) and 200 μg/mL of lysozyme, 5 mM $MgCl_2$, and 100 μg/mL of DNase I. After sonication, cell debris was removed by centrifugation for 45 min at 11 000 rpm at 4 °C. The supernatant was dialyzed against 20 mM TEA-HCl containing 300 mM NaCl, pH 7.8, for 2 h at 4 °C. After centrifugation, the supernatant was applied to a 50 mL Ni^{2+}-NTA affinity column (Novagen), and proteins were eluted with a linear 25−250 mM imidazole gradient at 1 mL/min. Active fractions were pooled, concentrated to 4 mL, and loaded onto a 1.6 cm × 70 cm Superdex 200 gel filtration column. The enzyme was eluted at 0.5 mL/min, and the active fractions were pooled.

Protein concentrations were measured using a Bio-Rad protein assay kit with bovine serum albumin as a standard. The subunit molecular mass of WT and mutants of PS was determined by SDS-PAGE according to the method of Laemmli (*20*). The native molecular mass was estimated by gel filtration chromatography. Electrospray ionization/mass spectrometry was performed on the purified enzymes to determine the subunit molecular mass of WT and mutants of PS.

Spectrophotometric Enzyme Assay. PS activity was assayed spectrophotometrically by coupling the formation of AMP to the reactions of myokinase, pyruvate kinase, and lactate dehydrogenase as previously described (*11*). Reaction mixtures contained 100 mM HEPES, pH 7.8, 10 mM $MgCI_2$, 10 mM ATP, 5 mM β-alanine, 5 mM D-pantoate, 1 mM potassium phosphoenolpyruvate, 200 μM NADH, 18 u myokinase, 18 u pyruvate kinase, and 18 u lactate dehydrogenase in a total volume of 1.0 mL at 25 °C. After incubation for 5 min at 25 °C, the reactions were initiated by the addition of PS (≤10 μL). The rate of Pan formation is proportional to the rate of NADH oxidation where two molecules of NADH are oxidized for each molecule of Pan formed. Initial velocity experiments were carried out at various concentrations of one substrate with the concentration of the other two substrates kept saturating and constant.

Isotopic Enzyme Assay. Enzyme activities were determined by an isotopic method using [^{14}C]β-alanine (*11*). Reaction mixtures contained 10 mM ATP, 5 mM sodium pantoate, 20−800 μM β-alanine (50 μCi/μmol), and 10 mM $MgCl_2$ in 100 mM HEPES, pH 7.5. The reaction was initiated by the addition of PS (≤10 μL). After incubation for 5−600 s at 25 °C, the reactions were stopped by the addition of 0.1 N HCl, by heating reaction mixtures in a boiling water bath for 1 min, and by pelleting the precipited enzyme by centrifugation. The supernatant was spotted onto PEI TLC plates, and radiolabeled β-alanine and Pan were separated using 0.3 M formic acid as the mobile phase. The amount of Pan formed was quantitated using a Phosphorimager (Molecular Dynamics) and corrected for nonenzymatic activity.

Presteady State Kinetics. Single turnover experiments for both the first and the second half reactions on both WT and mutant enzymes were performed as previously described (*11*).

Alkylation of K160C Mutant. Alkylation of the K160C mutant enzyme was performed as previously described (*21*). The reaction contained 20 mM TEA-HCl, pH 7.8, 50 mM bromoethylamine, and 3 mg of K160C in a total volume of 1.0 mL. After incubation for 1 h at 25 °C, the reaction mixture was dialyzed against 5 mM ammonium acetate at pH 6.5, and 1 mM DTT was added to remove residual bromoethylamine. The WT enzyme contained no cysteine residues, and its activity was unaffected by incubation with bromoethylamine.

Isothermal Titration Microcalorimetry. The thermodynamic studies of both WT and mutant enzymes were performed using a MCS microcalorimeter (Microcal, Inc., Northampton, MA). Enzymes were dialyzed against 50 mM HEPES, pH 7.5, containing 5 mM $MgCl_2$ at 4 °C, and the concentrations of the enzymes used in the experiments were 70−200 μM. ATP was dissolved in the same buffer to a concentration of 3−15 mM. In individual titration, injections of 7 μL of the ligand solution were made via the computer-controlled microsyringe into the 1.5 mL enzyme solution at an interval of 4 min, while being stirred at 300 rpm, at 27 °C. The data were fitted to a theoretical titration curve using software supplied by Microcal, Inc., with ΔH (the binding enthalpy change in kcal mol^{-1}), K_a (the binding constant in M^{-1}), and n (the number of binding sites per monomer) as adjustable parameters. The thermodynamic parameters ΔG and ΔS were calculated from eqs 5 and 6.

Data Analysis. Kinetic data were fitted to the appropriate rate equations by using the programs developed by Cleland (*22*). The initial velocity data were fitted to eq 1:

$$v = VA/(K_a + A) \quad (1)$$

where v is the reaction velocity, V is the maximal velocity, and K_a is the Michaelis constant for substrate A. The single turnover data were fitted to eq 2 (*24*).

$$Y = A\,(1 - e^{-k_{obs}t}) \quad (2)$$

For a two step binding mechanism, the dependence of the single exponential rate constant k_{obs} as a function of substrate concentration is given by eq 3 (*23*). For both PS half reactions, the intercept of k_{obs} vs substrate concentration curves appeared to be approximately zero, arguing that in eq 3, k_{rev} is zero. The data were thus fitted to eq 4:

$$k_{obs} = k_{for}[A]/(K_d + [A]) + k_{rev} \quad (3)$$

$$k_{max} = k_{for} + k_{rev}$$

$$k_{obs} = k_{max}[A]/(K_d + [A]) \quad (4)$$

where k_{obs} was calculated from eq 2 and k_{max} was the maximal rate of the half reaction at saturating [A]. The thermodynamic data were fitted to a theoretical titration curve using software supplied by Microcal, Inc. The thermodynamic parameters ΔG and ΔS were calculated from eqs 5 and 6:

$$\Delta G = -RT \ln K_a \quad (5)$$

$$\Delta G = \Delta H - T\Delta S \quad (6)$$

where K_a is the association constant; ΔG, ΔH, and ΔS are the free energy, enthalpy, and entropy, respectively, of ATP binding; T is the absolute temperature; and $R = 1.98$ cal mol^{-1} K^{-1}.

RESULTS

Mutagenesis, Expression, and Purification of Mutant PSs. Alanine mutations were introduced at residues His44, His47, Lys160, Asn69, Gln72, and Gln164, based on the three-dimensional structures of *M. tuberculosis* PS complexes with ATP, pantoate, and the pantoyl adenylate intermediate. Theses six residues are completely conserved in the amino acid sequence alignment of 13 microbial PSs (see Supporting Information). All mutations were confirmed by nucleotide sequencing. All mutants of PS were expressed in *E. coli* BL21(DE3) cells at 18 °C and purified to homogeneity in a yield of 200−300 mg from 8 to 10 g of *E. coli* cells using Ni^{2+}-NTA affinity and Superdex 200 gel filtration chromatography. The subunit molecular mass of PS determined by SDS-PAGE is ∼33 kDa.

Steady State Kinetic Studies. The kinetic parameters of WT and mutant forms of *M. tuberculosis* PS were determined by initial velocity experiments using both the spectrophotometric, coupled enzyme assay and the isotopic assay. The k_{cat} values of theses mutants were determined to be 0.5−15% that of the WT enzyme using the coupled enzyme assay, which monitors AMP formation (Table 1). However, using the isotopic assay to directly monitor Pan formation, the PS

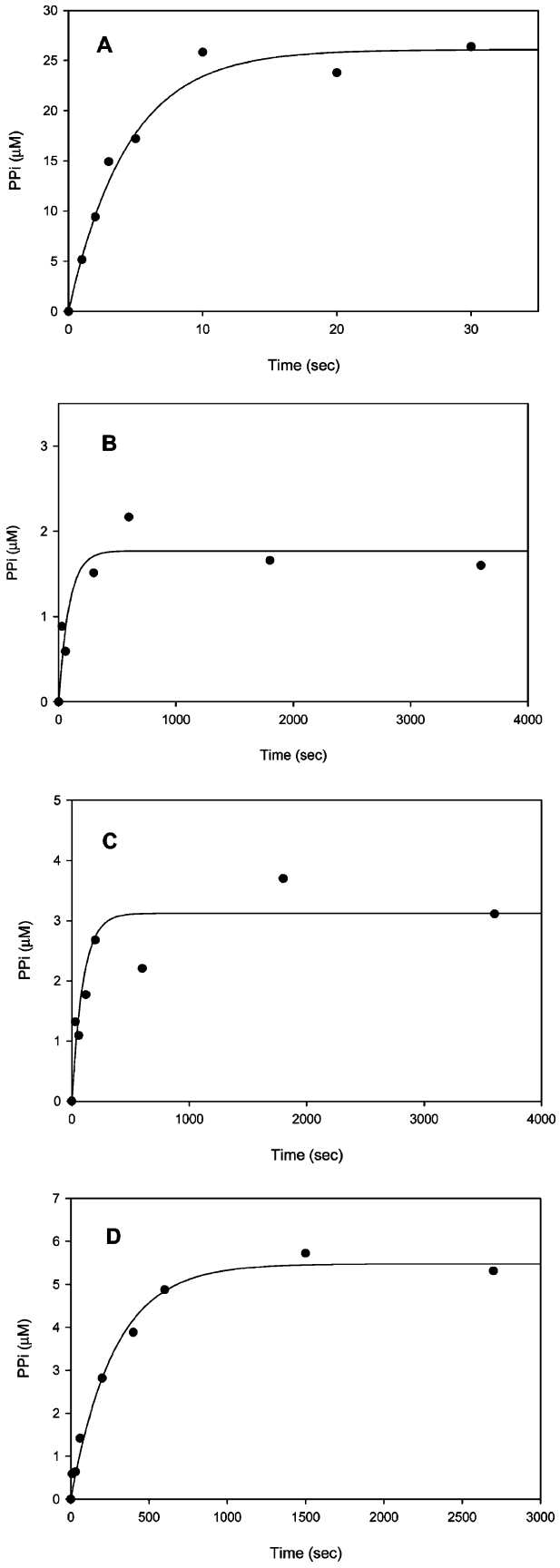

FIGURE 1: Time courses of pyrophosphate formation. Reactions catalyzed by WT (A), H44A (B), H47A (C), and Q164A (D) PS. Reaction mixtures contained 28 μM PS, 10 mM sodium pantoate, 800 μM [γ-^{32}P]ATP (20 μCi/μmol), and 10 mM $MgCl_2$ in 100 mM HEPES, pH 7.8, at 25 °C. The smooth curves are fits of the data to eq 2.

Table 2: Presteady State Kinetic Parameters for WT and Mutants of PS

PS	pyrophosphate formation in the first half reaction		Pan formation in the second half reaction	
	k_{max} (s^{-1})	$K_{d,ATP}$ (mM)	k_{max} (s^{-1})	$K_{d,\beta-ala}$ (mM)
WT	1.3 ± 0.3	1.8 ± 0.5	2.6 ± 0.3	0.7 ± 0.1
H44A	0.025 ± 0.007	0.6 ± 0.3	<0.001	
H47A	0.022 ± 0.004	0.3 ± 0.1	<0.001	
K160A	<0.001			
K160C	<0.001			
$K160C_{-CH_2CH_2NH_2}$	0.011 ± 0.002	0.4 ± 0.1	<0.001	
Q164A	0.045 ± 0.010	1.7 ± 0.5	0.066 ± 0.006	0.09 ± 0.03
N69A	0.025 ± 0.015	1.8 ± 0.7	<0.001	
Q72A	0.029 ± 0.005	0.7 ± 0.2	<0.001	

activity of all mutants (except Q164A) was at least 1000-fold less than the WT enzyme (Table 1). The same, affinity-purified enzyme preparations were used in both studies, arguing against contamination of the preparations with WT Pan synthase. To determine the source of this discrepancy between the two steady state analyses, we determined the competence of the mutant enzymes to catalyze each of the two isolated half reactions.

Presteady State Kinetics. The rate of pyrophosphate formation in the first half reaction was determined by single turnover experiments using rapid quench techniques with [γ-^{32}P]ATP, in the absence of β-alanine (*11*). Plots of pyrophosphate concentration vs time were obtained at different concentrations of [γ-^{32}P]ATP (Figure 1). The data were fitted to eq 2 to obtain the rate constants at each [ATP]. The rate constant for each reaction was subsequently plotted as a function of [ATP] and fitted to eq 4 to obtain the maximum value for the rate constant. The maximal rates of pyrophophate formation for H44A, H47A, N69A, Q72A, and Q164A are lower than that for WT enzyme by 28−50-fold (Table 2). The enzyme activity of K160A and K160C mutants was too low to be determined. The apparent internal equilibrium constant ([E•HP-AMP•PP_i]/[E•HP•ATP]) was 2 for WT enzyme, 0.3 for Q164A, and ca. 0.05 for H47A (Figure 2).

The rate of Pan formation in the second half reaction was measured in a similar manner. Plots of [Pan] formed vs time were generated using different concentrations of [^{14}C]β-alanine. The data were fitted to eq 2 to obtain the rate constant at each [β-alanine]. The rate of each reaction was subsequently plotted as a function of [β-alanine] and fitted to eq 4 to obtain the maximum value for the rate constant (Table 2). The rate of Pan formation for the Q164A mutant was decreased 39-fold as compared to that for WT enzyme. However, Pan formation could not be detected for the H44A, H47A, K160A, K160C, N69A, and Q72A mutants (Table 2).

Chemical Rescue of the K160C Mutant by Aminoethylation. Replacement of the Lys160 residue with cysteine resulted in a mutant form whose steady state activity was equivalent to the K160A mutant. The activity of the K160C mutant was markedly increased by the alkylation of K160C with bromoethylamine (Figure 3 and Tables 1 and 2).

Isothermal Titration Microcalorimetry. Thermodynamic parameters of ATP binding to WT *M. tuberculosis* PS and site-directed mutants were determined by isothermal titration microcalorimetry and are listed in Table 3. As compared with the WT enzyme, the association constants for ATP to K160A and H47A are decreased ∼50 and ∼10-fold, respectively, while those for N69A, Q72A, and Q164A are not significantly changed (∼2-fold or less). The enthalpy of ATP binding, ΔH, ranged from −17.3 to −13.0 kcal/mol for WT, Q164A, Q72A, and N69A enzymes and from −8.4 to −7.2 for K160A and H47A (Table 3). The $T\Delta S$ values for the binding of ATP to WT, N69A, Q72A, and Q164A are large and negative, whereas the $T\Delta S$ values for H47A and K160A are small. No significant changes in the overall binding energy, ΔG, were observed between WT and Q164A, Q72A, and N69A. As compared to the WT enzyme, the ΔG values determined for K160A and H47A are significantly changed by −2.3 and −1.3 kcal mol^{-1}, respectively. Thermodynamic data for the H44A mutant were not obtained due to precipitation of this mutant enzyme during the experiment.

DISCUSSION

Steady State Kinetics. The three-dimensional structures of *M. tuberculosis* PS complexes with substrates and the pantoyl adenylate intermediate (*15*) have revealed that several active site residues interact with ATP, pantoate, and an adenylate intermediate (Figure 4). These residues are strictly conserved in the aligned amino acid sequences of 13 PSs (Supporting Information). Of these, H44, H47, and K160 interact directly or via water molecules with ATP, while N69, Q72, and Q164 residues interact via hydrogen bonds with pantoate (*15*). In the mechanistically related malonyl-CoA synthetase, both steady state kinetic and structural studies revealed the involvement of similarly conserved lysine and histidine residues in the formation of an malonyl-adenylate intermediate (*24*). We mutated six active site residues, H44, H47, N69, Q72, K160, and Q164, to alanine and examined whether their catalytic effectiveness was affected by these mutations. Low, but measurable, PS enzyme activity (0.5−15% that of the WT enzyme) was observed for these six mutant enzymes in the coupled spectrophotometric enzyme assay that monitors the formation of AMP. These activities seemed high for mutants in which key catalytic residues were removed, and we sought an independent measurement for overall activity, i.e., the formation of Pan. Using the direct isotopic assay to monitor Pan formation, we were unable to demonstrate activity for the H44A, H47A, N69A, Q72A, or K160A mutants. A possible explanation for this discrepancy was that these mutants slowly generated the pantoyl adenylate intermediate but released this normally tightly bound intermediate. In solution, the intermediate would rapidly lactonize (*25*) to release pantoyl lactone and AMP (Scheme 2). The spectrophotometric assay, which measures AMP formation, would

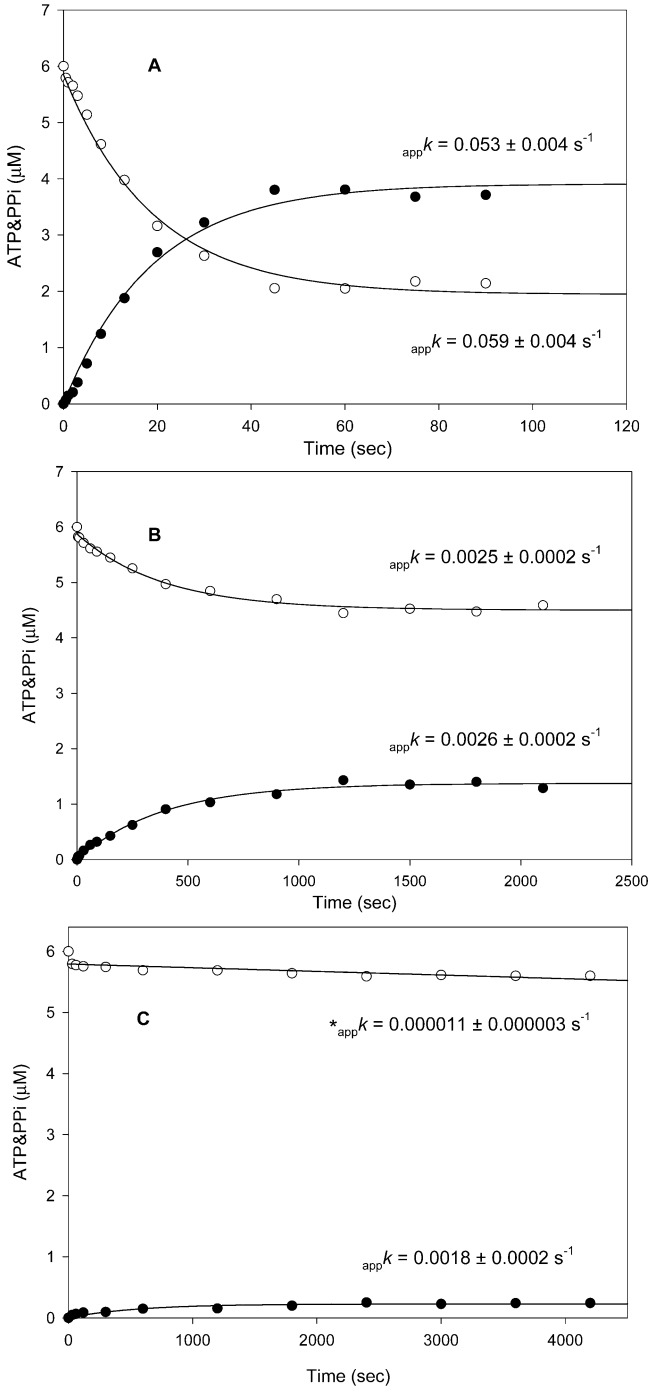

FIGURE 2: Equilibrium constant of adenylate formation. Time courses for ATP consumption (○) and pyrophosphate formation (●) catalyzed by WT (A), Q164A (B), and H44A (C) mutants. The reaction mixture contains 30 μM PS, 6 μM ATP, 10 mM sodium pantoate, and 10 mM $MgCl_2$ at 25 °C in 100 mM HEPES, pH 7.8. The smooth curves are fits of the data to eq 2. For the H44A mutant, the change in [ATP] was too small to get reliable rate constant information.

thus be reporting only on the first half reaction in this case, rather than the tightly coupled formation of Pan after reaction of β-alanine with the adenylate. In support of this interpretation, for both the WT and the Q164A mutant, AMP formation is absolutely dependent on added β-alanine, while for both the H44A and the Q72A mutants, AMP formation is observed in steady state, spectrophotometric measurements in the absence of β-alanine (data not shown). To confirm this, we performed single turnover experiments.

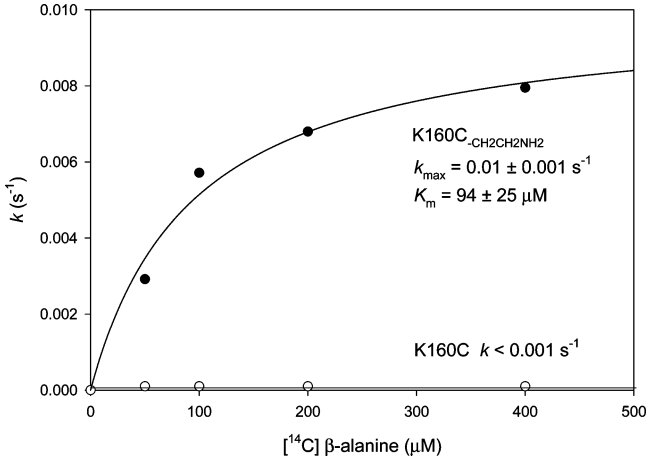

FIGURE 3: PS activity exhibited by the K160C mutant after (●) and before (○) treatment with bromoethylamine.

Table 3: Thermodynamic Parameters of ATP Binding to WT and Mutant PS[a]

PS	K_a ($\times 10^4$ M^{-1})	$-\Delta H$ (kcal mol^{-1})	$-\Delta G$ (kcal mol^{-1})	$-T\Delta S$ (kcal mol^{-1})
WT	22.4 ± 1.6	14.2 ± 0.2	7.3	6.9
Q164A	13.2 ± 0.29	17.3 ± 0.1	7.0	10.3
Q72A	13.1 ± 1.3	13.1 ± 0.46	7.0	6.1
N69A	9.1 ± 0.4	13.0 ± 0.23	6.8	6.2
H47A	2.46 ± 0.11	7.2 ± 0.2	6.0	1.2
K160A	0.45 ± 0.02	8.4 ± 0.3	5.0	3.4

[a] Conditions: 130−250 μM enzymes, 2−15 mM ATP, 5 mM $MgCl_2$, and 50 mM HEPES, pH 7.5, at 300 K.

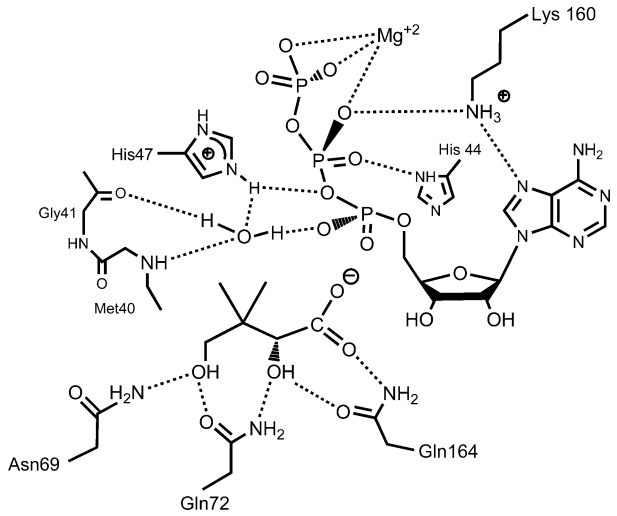

FIGURE 4: Active site structure of PS showing bound ATP and pantoate. The interactions between the residues mutated in this study and these substrates has been adapted from refs *14* and *15*.

Presteady State Kinetics. We have previously determined single turnover kinetics for both the first and the second half reactions on WT enzyme using rapid quench techniques (*11*). The maximum rate of pantoyl adenylate formation in the absence of β-alanine was 1.3 s^{-1}, and the maximum rate of synthesis of Pan from the pantoyl adenylate in the second step was 2.6 s^{-1}. These two half reactions are tightly coupled, and the pantoyl adenylate is tightly bound by the WT enzyme. In the present study, single turnover experiments for both the first and the second half reactions were performed on the mutant enzymes to examine which of these

two half reactions was impaired by the alanine substitutions in PS.

The conserved HxGH sequence has been reported to be part of the ATP-binding motif in the cytidylyltransferase superfamily of enzymes (*14*). In the three-dimensional structure of the *M. tuberculosis* PS-AMP-CPP complex (*15*), the imidazole ring of His44 makes a hydrogen bond with the β-phosphate group of AMP-CPP, while the imidazole ring of His47 is ~3.4 Å from the carbon atom between the α- and the β-phosphate of AMP-CPP (Figure 4). On the basis of this structure, the authors proposed that His 47 functions as a general acid to donate a proton to the leaving pyrophosphate, facilitating the formation of adenylate intermediate (*15*). Replacement of His 47 with Ala leads to a 59-fold decrease in the k_{max} value, suggesting that the adenylation step is compromised by this replacement and supporting the functional interpretation of the crystal structure (*15*). It has also been documented that His45, equivalent to H47, of tyrosyl-tRNA synthetase, another member of the acyl-adenylate forming enzyme family, plays an important role in the formation of a tyrosyl-AMP intermediate and the stabilization of the transition state (*26*). The k_{max} value for the pantoyl adenylate formation catalyzed by the H44A mutant was also 52-fold lower than that of the WT enzyme (Table 2).

The conserved Lys residue has been shown to be important for enzyme activity in the acyl-adenylate forming enzyme family (*27*) and has been proposed to participate in an electrostatic interaction with the negatively charged phosphate group of ATP (*28*). Lys160 of *M. tuberculosis* PS was observed to interact with the β-phosphate group of AMP-CPP in the crystal structure (*15*). The mutation of Lys160 to Ala resulted in the abolishment of the adenylation activity, confirming the importance of the Lys160 residue in the formation of the pantoyl adenylate intermediate.

Structural studies of both the *E. coli* and the *M. tuberculosis* synthetases have also revealed that the C2 and C4 hydroxyl groups and carboxyl oxygen of the pantoate molecule interact with side chains of Asn69, Gln164, and Gln72 (*14*, *15*). The N69A, Q72A, and Q164A mutants exhibited poor activity (29−52-fold lower than that of WT PS) in the adenylation step, suggesting that these three active site residues are also essential for pantoate binding and the formation of the pantoyl adenylate intermediate. All of these single turnover studies of the adenylation reaction catalyzed by the mutant forms of the enzyme essentially mirror the results obtained using the coupled spectrophotometric assay.

The adenylation half reaction for the WT enzyme and Q164A and H44A mutants in single turnover experiments showed that the ratio of the pyrophosphate to ATP at the completion of the first half reaction was significantly decreased from 2.0 for WT to 0.3 for Q164A and ca. 0.05 for H44A mutant (Figure 2). This half reaction is known to be readily reversible from isotope exchange experiments (*11*). The decreased equilibrium constant suggested that the loss of a hydrogen bond to either ATP or pantoate results in an apparently impaired ability to stabilize the pantoyl adenylate intermediate at the active site. In the case of 4-CBA:CoA ligase, mutation of active site residues caused a similar decrease in the internal equilibrium constant ascribed to a decrease in the ability to stabilize the acyl-adenylate intermediate (*29*).

We were unable to measure the rate of the second half reaction (formation of Pan and decomposition of adenylate) in the single turnover experiment using five out of the six mutants. The Q164A mutant exhibited a lowered activity (39-fold lower than that of WT enzyme; Table 2), consistent with the results obtained from the steady state measurement using the isotopic assay. Our inability to demonstrate the second half reaction could be due to this reaction also being compromised in these mutant forms of the enzyme or a combination of the very slow rates of the two half reactions coupled to the slow release of the adenylate. The release of the adenylate would prevent the establishment of an equilibrium for the first half reaction, as is observed with the H44A mutant (Figure 2C).

Chemical Rescue of K160C Mutant by Alkylation of Cysteine. The K160C mutant showed an extremely low activity in both steady state and presteady state (adenylation) kinetics. The activity of the K160C mutant can be increased 10-fold by alkylation with bromoethylamine in both steady state and presteady state reactions (Tables 1 and 2). These data suggested that the amino group of chemically generated 4-thia-K160 can restore the function of the K160C mutant, supporting the essential role of K160 in the formation of pantoyl adenylate intermediate.

Isothermal Titration Microcalorimetry. The binding constants and thermodynamic parameters associated with ATP binding to the WT and mutant PSs are shown in Table 3. The H47A and K160A mutant enzymes exhibited 10- and 50-fold decreases in K_a values. On the basis of the crystal structure, the H47A and K160A mutants are expected to lose one hydrogen bond to the ATP molecule. The loss of this hydrogen bond is probably the dominant factor in any changes to the thermodynamics of ATP binding. The loss of a hydrogen bond is generally expected to result in decreases in the enthalpy of binding and a compensating favorable change in entropy (*30*, *31*).

The Q72A and N69A mutations have essentially no effect on the thermodynamic parameters of ATP binding. The Q164A has an unusual and structurally unpredicted effect, exhibiting a more negative ΔH and compensatory higher $T\Delta S$ for ATP binding. The explanation for this altered pattern of enthalpic and entropic contributions to ATP binding in this mutant is under investigation.

In summary, the results presented in this study, along with three-dimensional structure analysis of *E. coli* and *M. tuberculosis* PSs (*14*, *15*), demonstrate that the highly conserved active site residues, H44, H47, N69, Q72, K160, and Q164, play important functional roles in substrate binding and catalysis of the adenylation step in the PS reaction. These six conserved residues make important interactions with a pantoyl adenylate and are required for the stabilization of this highly reactive intermediate at the active site, suggesting that a nonreactive analogue of pantoyl adenylate would be a specific inhibitor for PS.

SUPPORTING INFORMATION AVAILABLE

Figure showing the sequence alignment of 13 PSs. This material is available free of charge via the Internet at http://pubs.acs.org.

REFERENCES

1. Neidhardt, F. (1996) *Escherichia coli and Salmonella typhimurium: Cellular and Molecular Biology*, 2nd ed., pp 687−694, American Society for Microbiology, Washington, DC.
2. Abiko, Y. (1975) Metabolism of coenzyme A, In *Metabolic Pathways* (Greenburg, D. M., Ed.), pp 1−25, Academic Press, Inc., New York.
3. Dreier, J., Shah, A. N., and Khosla, C. (1999) Kinetic analysis of the actinorhodin aromatic polyketide synthase, *J. Biol. Chem. 274*, 25108−25112.
4. Lambalot, R. H., Gehring, A. M., Flugel, R. S., Zuber, P., LaCelle, M., Marahiel, M. A., Reid, R., Khosla, C., and Walsh, C. T. (1996) A new enzyme superfamily−the phosphopantetheinyl transferases, *Chem. Biol. 3*, 923−936.
5. Maas, W. K., and Vogel, H. J. (1953) α-Ketoisovaleric acid, a precursor of pantothenic acid in *Escherichia coli*, *J. Bacteriol. 65*, 388−393.
6. Brown, G. M., and Williamson, J. M. (1982) Biosynthesis of riboflavin, folic acid, thiamine, and pantothenic acid, *Adv. Enzymol. 53*, 345−381.
7. Cronan, J. E., Jr., Littel, K. J., and Jackowski, S. (1982) Genetic and biochemical analyses of pantothenate biosynthesis in *Escherichia coli* and *Salmonella typhimurium*, *J. Bacteriol. 149*, 916−922.
8. Brown, G. M., and Williamson, J. M. (1987) In *Escherichia coli and Salmonella typhimurium: Cellular and Molecular Biology* (Neidhardt, F., Ingraham, J. L., Low, K. B., Magasanik, B., Schaechter, M., and Umbarger, H. E., Eds.) pp 521−538, American Society for Microbiology, Washington, DC.
9. Sambandamurthy, V. K., Wang, X., Chen, B., Russell, R. G., Rerick, S., Collins, F. M., Morris, S. L., and Jacobs, W. R. (2002) A pantothenate auxotroph of *Mycobacterium tuberculosis* is highly attenuated and protects mice against tuberculosis. *Nat. Med. 8*, 1171−1174.
10. Miyatake, K., Nakano, Y., and Kitaoka, S. (1979) Pantothenate synthetase from *Escherichia coli* [D-pantoate: β-alanine ligase (AMP-forming), EC 6.3.2.1], *Methods Enzymol. 62*, 215−219.
11. Zheng, R., and Blanchard, J. S. (2001) Steady-state and pre-steady-state kinetic analysis of *Mycobacterium tuberculosis* pantothenate synthetase, *Biochemistry 40*, 12904−12912.
12. Miyatake, K., Nakano, Y., and Kitaoka, S. (1978) Enzymological properties of pantothenate synthetase from *Escherichia coli* B, *J. Nutr. Sci. Vitaminol. 24*, 243−253.
13. Genschel, U., Powell, C. A., Abell, C., and Smith, A. G. (1999) The final step of pantothenate biosynthesis in higher plants: cloning and characterization of pantothenate synthetase from *Lotus japonicus* and *Oryza sativum* (rice), *Biochem. J. 341*, 669−678.
14. von Delft, F., Lewendon, A., Dhanaraj, V., Blundell, T. L., Abell, C., and Smith, A. G. (2001) The crystal structure of *E. coli* pantothenate synthetase confirms it as a member of the cytidylyltransferase superfamily, *Structure 9*, 439−450.
15. Wang, S., and Eisenberg, D. (2003) Crystal structures of a pantothenate synthetase from *M. tuberculosis* and its complexes with substrates and a reaction intermediate, *Protein Sci. 12*, 1097−1108.
16. Williams, L., Zheng, R., Blanchard, J. S., and Raushel, F. M. (2003) Positional isotope exchange analysis of the pantothenate synthetase reaction, *Biochemistry 42*, 5108−5113.
17. Kim, Y. S., and Kang, S. W. (1994) Steady-state kinetics of malonyl-CoA synthetase from *Bradyrhizobium japonicum* and evidence for malonyl-AMP formation in the reaction, *Biochem. J. 297*, 327−333.
18. Kisselev, L. L., and Favorova, O. O. (1974) Aminoacyl-tRNA synthetases: sone recent results and achievements, *Adv. Enzymol. 40*, 141−238.
19. King, H. L., Jr., Dyar, R. E., and Wilken, D. R. (1974) Ketopantoyl lactone and ketopantoic acid reductases. Characterization of the reactions and purification of two forms of ketopantoyl lactone reductase, *J. Biol. Chem. 249*, 4689−4695.
20. Laemmli, U. K. (1970) Cleavage of structural proteins during the assembly of the head of bacteriophage T4, *Nature 227*, 680−685.
21. Piotrowski, J., Beal, R., Hoffman, L., Wilkinson, K. D., Cohen, R. E., and Pickart, C. M. (1997) Inhibition of the 26S proteasome by polyubiquitin chains synthesized to have defined lengths, *J. Biol. Chem. 272*, 23712−23721.
22. Cleland, W. W. (1979) Statistical analysis of enzyme kinetic data, *Methods Enzymol. 63*, 103−138.
23. Johnson, K. A. (1992) Transient-State Kinetic Analysis of Enzyme Reaction Pathways, in *The Enzymes*, 3rd ed., (Sigman, D. S., Ed.) Vol. 20, pp 1−60, Academic Press: New York.
24. An, J. H., Lee, G. Y., Jung, J. W., Lee, W., and Kim, Y. S. (1999) Identification of residues essential for a two-step reaction by malonyl-CoA synthetase from *Rhizobium trifolii*, *Biochem. J. 344*, 159−166.
25. Pfleiderer, G., Kreiling, A., and Wieland, T. (1960) On pantothenic acid synthetase from *E. coli*. I. Concentration with the aid of an optical test, *Biochem. Z. 333*, 302−307.
26. Leatherbarrow, R. J., and Fersht, A. R. (1987) Investigation of transition-state stabilization by residues histidine-45 and threonine-40 in the tyrosyl-tRNA synthetase, *Biochemistry 26*, 8524−8528.
27. Kim, I. Y., Veres, Z., and Stadtman, T. C. (1993) Biochemical analysis of *Escherichia coli* selenophosphate synthetase mutants. Lysine 20 is essential for catalytic activity and cysteine 17/19 for 8-azido-ATP derivatization, *J. Biol. Chem. 268*, 27020−27025.
28. Saraste, M., Sibbald, P. R., and Wittinghofer, A. (1990) The P-loop−a common motif in ATP- and GTP-binding proteins, *Trends Biochem. Sci. 15*, 430−434.
29. Chang, K., Xiang, H., and Dunaway-Mariano, D. (1997) Acyl-adenylate motif of the acyl-adenylate/thioester-forming enzyme superfamily: A site-directed mutagenesis study with the *Pseudomonas* sp. strain CBS3 4-chlorobenzoate: Coenzyme A ligase, *Biochemistry 36*, 15650−15659.
30. Hawkes, R., Grutter, M. G., and Schellman, J. (1984) Thermodynamic stability and point mutations of bacteriophage T4 lysozyme, *J. Mol. Biol. 175*, 195−212.
31. Shortle, D., Meeker, A. K., and Freire, E. (1988) Stability mutants of staphylococcal nuclease: large compensating enthalpy−entropy changes for the reversible denaturation reaction, *Biochemistry 27*, 4761−4768.

BI049676N